

Dynamic segmentation and linear prediction for maternal ECG removal in antenatal abdominal recordings

R Vullings¹, C H L Peters², R J Sluijter¹, M Misch¹, S G Oei³ and J W M Bergmans¹

¹ Department of Electrical Engineering, Eindhoven University of Technology, Eindhoven, The Netherlands

² Department of Clinical Physics, Amphia Hospital, Breda, The Netherlands

³ Department of Obstetrics and Gynecology, Máxima Medical Center, Veldhoven, The Netherlands

E-mail: R.Vullings@tue.nl

Received 14 October 2008, accepted for publication 13 January 2009

Published 17 February 2009

Online at stacks.iop.org/PM/30/291

Abstract

Monitoring the fetal heart rate (fHR) and fetal electrocardiogram (fECG) during pregnancy is important to support medical decision making. Before labor, the fHR is usually monitored using Doppler ultrasound. This method is inaccurate and therefore of limited clinical value. During labor, the fHR can be monitored more accurately using an invasive electrode; this method also enables monitoring of the fECG. Antenatally, the fECG and fHR can also be monitored using electrodes on the maternal abdomen. The signal-to-noise ratio of these recordings is, however, low, the maternal electrocardiogram (mECG) being the main interference. Existing techniques to remove the mECG from these non-invasive recordings are insufficiently accurate or do not provide all spatial information of the fECG. In this paper a new technique for mECG removal in antenatal abdominal recordings is presented. This technique operates by the linear prediction of each separate wave in the mECG. Its performance in mECG removal and fHR detection is evaluated by comparison with spatial filtering, adaptive filtering, template subtraction and independent component analysis techniques. The new technique outperforms the other techniques in both mECG removal and fHR detection (by more than 3%).

Keywords: fetal electrocardiogram, QRS-detection, template subtraction

1. Introduction

Currently the most widespread method to monitor fetal health is cardiotocography (CTG) (Dawes *et al* 1981), which consists of the simultaneous monitoring of the fetal heart rate (fHR) and maternal uterine activity. However, in many cases the CTG does not provide conclusive information for accurate assessment of fetal health and, therefore, additional information is needed for clinical decision-making (Amer-Wahlin *et al* 2001, Thacker *et al* 2006).

The main additional sources of information to support the CTG are micro-blood examination and fetal electrocardiogram (fECG) analysis using an invasive electrode. Both these methods require invasive measurements and consequently can only be applied during labor and entail an increased risk of infection. The spectral analysis of the fHR can also offer additional information (Van Laar *et al* 2008, Siira *et al* 2005). If this is performed on non-invasively determined fHR, it can be applied in stages of pregnancy earlier than labor.

The non-invasive fHR is generally determined by means of Doppler ultrasound. This method, however, does not allow long-term monitoring since it is sensitive to maternal and fetal motion, resulting in a relatively low signal-to-noise ratio (SNR), and since the ultrasound transducers transmit energy into the fetal body, potentially endangering fetal health.

To overcome low SNR problems, in modern CTG devices a buffer of consecutive heart beats is autocorrelated at constant frequency to provide a reliable, but slightly smoothed, fHR signal. Although this fHR measurement approaches the ‘gold standard’ of the fHR determined from an invasively recorded fetal ECG (Lawson *et al* 1983), particularly the high frequency parameters in the spectral analysis of the fHR are affected by the smoothing of the autocorrelation method.

From this it is clear that any non-invasive method to support the CTG, resolving the problems associated with Doppler ultrasound, can be highly valuable. One such method is fECG monitoring with abdominal electrodes. Besides the fECG, this method also enables accurate spectral analysis of the unsmoothed fHR, i.e., it can provide the fHR on a beat-to-beat basis, and due to its passive nature and relative insensitivity to fetal motion it can be used for long-term monitoring. In addition to improved spectral analysis of the fHR, the abdominally recorded fECG also enables analysis of the fECG. Relative changes in the segments and intervals of the fECG are associated with fetal distress (Greene *et al* 1982) and growth (Stinstra *et al* 2002), implying that fECG monitoring provides additional information on the fetal condition.

The fECG recorded from the maternal abdomen is affected by noise consisting of a mixture of several interferences. As, in general, the maternal electrocardiogram (mECG) is the predominant interference (Bemmel and van der Weide 1966), several techniques for mECG removal from the abdominal signals are presented in literature (Bergveld and Meijer 1981, Widrow *et al* 1975, Strobach *et al* 1994, Cerutti *et al* 1986, Ungureanu and Wolf 2006, Ungureanu *et al* 2007, Martens *et al* 2007, Comani *et al* 2004, De Lathauwer *et al* 2000). However, none of these techniques can remove the mECG completely or extract the fECG (Zarzoso and Nandi 2001) as the interferences in the abdominal recordings do not completely satisfy the assumptions implicitly made by the presented techniques.

Therefore, in this paper a new technique is presented for the removal of the mECG. This technique is an extension of mECG template subtraction techniques (Cerutti *et al* 1986, Ungureanu and Wolf 2006, Ungureanu *et al* 2007, Comani *et al* 2004) and is referred to as the weighted averaging of mECG segments (WAMES). WAMES operates by dynamically dividing the mECG complex in separate segments and generating an estimate for each individual segment. Each estimate is hereby obtained by the linear combination of time-shifted, offset compensated and scaled corresponding segments in preceding mECG complexes. This process

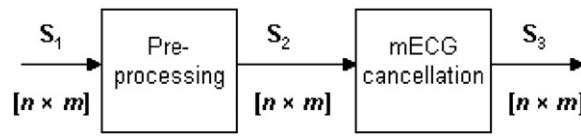


Figure 1. Schematic view of fECG extraction techniques.

can also be viewed as a dynamic segmentation and linear prediction of mECG segments. By time aligning, offset compensating and scaling the individual segments before linearly combining them, morphological variations in the mECG complex can be dealt with accurately since the only assumption of WAMES is a quasi-periodicity of the mECG segments. This is in contrast to other template subtraction techniques, which assume a larger degree of periodicity in the mECG.

WAMES is evaluated in terms of mECG estimation and fHR detection. Its performance is quantified on both modeled and real antenatal abdominal recordings, and compared to the performance of spatial filtering (Bergveld and Meijer 1981), adaptive filtering (Strobach *et al* 1994), template subtraction techniques (Ungureanu and Wolf 2006, Ungureanu *et al* 2007) and independent component analysis (ICA) (Zarzoso and Nandi 2001, Taylor *et al* 2003).

In section 2 this new technique is described. Section 3 is devoted to the other techniques for comparison and validation. Section 4 discusses the abdominal recordings used for the comparison and details on the methodology of this comparison. Finally, section 5 discusses the results and in section 6 our conclusions are drawn.

2. Dynamic segmentation and linear prediction for maternal ECG removal

Antenatal abdominal recordings generally constitute a mixture of fECG, mECG and noise such as motion artifacts, muscular activity and powerline interference. Consequently, most fECG extraction techniques operate by means of consecutive removal of each interference. Schematically, this can be seen as the two step procedure in figure 1, in which removal of motion artifacts, muscular activity and powerline interference is referred to as preprocessing. This preprocessing block is detailed in section 4. The abdominal recordings are represented in figure 1 by S_1 , which is a $[n \times m]$ matrix with n the number of electrodes on the maternal abdomen and m the number of samples in the recording. The preprocessed signals S_2 are subsequently fed into the mECG cancellation block; for WAMES this block is shown schematically in figure 2. Commonly, ECG complexes consist of a P-wave, a QRS complex (which can be subdivided into a separate Q-wave, R-wave and S-wave) and a T-wave (Guyton and Hall 2000) (figure 3). Each mECG complex in S_2 is segmented by the mECG segmentation block in figure 2 into individual waves, i.e., a separate P-, Q-, R-, S- and T-wave. Each segment is subsequently estimated by linear prediction, using corresponding segments from preceding mECG complexes. These estimated segments are finally combined to generate an estimate \hat{S}_2 of the mECG signal.

2.1. Dynamic maternal ECG segmentation

At a certain distance the heart can be modeled by a time-dependent dipole with variable amplitude and orientation (Plonsey 1969). In this framework, the ECG can be seen as the projection of the electrical field generated by this dipole on the measurement vector.

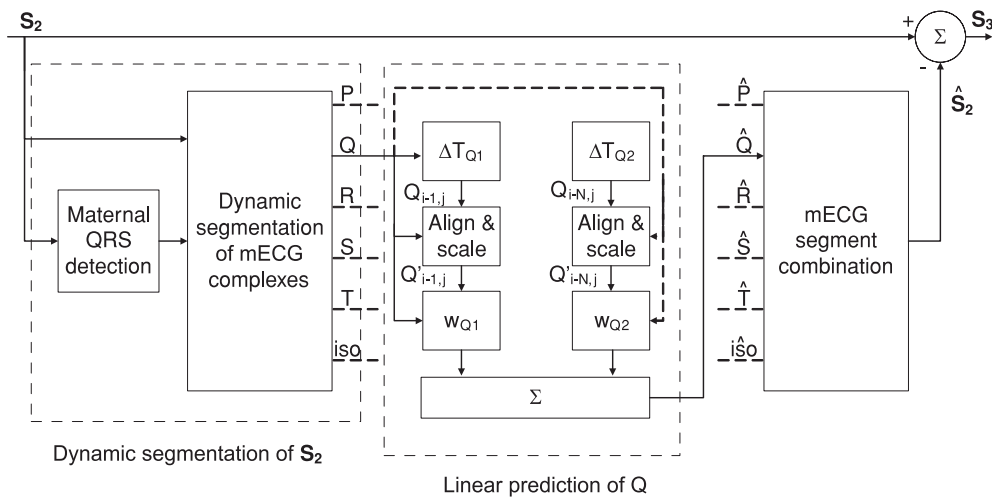


Figure 2. Block scheme of the mECG cancellation by WAMES. The delays $\Delta T_{Q1} \dots \Delta T_{QN}$ correspond to the time intervals between the Q-wave that is estimated and N preceding Q-waves. These time intervals are approximated in the maternal QRS detection block, in which the time intervals between consecutive R-waves are determined. Part of this scheme has been adopted from Martens *et al* (2007).

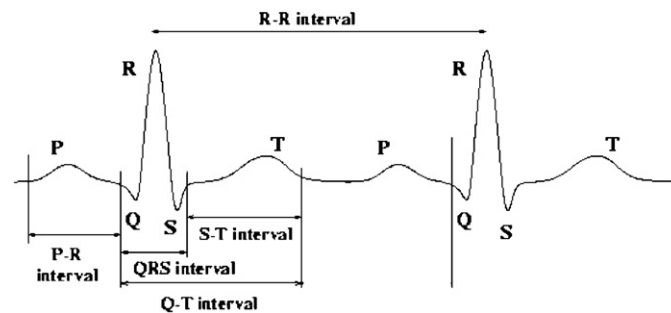


Figure 3. ECG nomenclature.

Respiration causes motion of the maternal abdomen and as a result the orientation of the measurement vector with respect to this electrical field varies over time. As each wave in the ECG exhibits its own orientation of the dipole, this variation is not proportional for each wave and therefore causes variability in the morphology of the ECG.

This morphological variability is the main reason for inaccuracies in existing template subtraction techniques. The template is not capable of accounting for all variations and consequently residuals of the mECG remain after subtraction of the template. These residuals can have amplitudes that exceed the amplitude of the fECG and therefore affect fHR detection. By generating a template for each individual wave the morphological variability can be accounted for more accurately, resulting in an improved mECG subtraction.

The segmentation of the mECG is performed in two steps. In the first step the signals are divided into individual mECG complexes, based on the locations of the QRS complexes, and in the second step each mECG complex is subdivided into the individual waves.

2.1.1. Maternal QRS detection. Depending on the position of the electrode on the maternal abdomen with respect to the position of the heart, some of the waves in figure 3 can be difficult to distinguish. Therefore, to facilitate the detection of maternal QRS complexes, the SNR of the maternal QRS complexes is enhanced by linearly combining the signals \mathbf{S}_2 in such way as to maximize the variance (principal component analysis, PCA) (Martens *et al* 2005). The linear combination with maximum variance is referred to as the principal component ζ .

Maternal QRS complexes are detected in ζ as local extrema that exceed an adaptive threshold μ . This method is adapted from Gritzali *et al* (1989), but with an adaptive threshold rather than a fixed threshold. This adaptive threshold is updated continuously by means of a Kalman filter and depends on the SNR of the maternal QRS complexes in ζ ; when the SNR changes the threshold is adapted to prevent noise from exceeding it. This Kalman filter is defined as

$$\mu_t = \mu_{t-1} + K_t(v_t - \mu_{t-1}), \quad (1)$$

with v_t the instantaneous threshold value at time t defined as

$$v_t = \xi \max\{|\zeta_{t-\tau}|, \dots, |\zeta_t|\}, \quad (2)$$

with ξ a parameter set at 0.6 based on the data and τ a time interval corresponding to the interval between the two last detected QRS complexes. The Kalman gain K_t is defined as

$$K_t = \frac{\rho_t^2}{\rho_t^2 + \sigma_\zeta^2}, \quad (3)$$

with

$$\rho_t^2 = \frac{\rho_{t-1}^2 \sigma_\zeta^2}{\rho_{t-1}^2 + \sigma_\zeta^2} \quad (4)$$

the variance of the estimate of μ_t at time t and σ_ζ^2 the variance of ζ in the interval $[t - \tau, t]$. The initial value of ρ_t^2 is set equal to the variance of $|\zeta|$ in the interval $[0, 2]$, i.e., the first 2 s of the principal component. This interval is chosen so as to ascertain inclusion of at least one maternal QRS complex, i.e., the maternal heart rate is assumed to exceed 30 beats per minute (BPM).

2.1.2. Dynamic segmentation of maternal ECG complexes. The segmentation of mECG complexes is performed in two steps. In the first step for each wave a window is defined in which the wave is assumed to be present; in the second step the wave is detected in this particular window. Hereby each window is defined by its onset and its width which are both based on a physiological model and shown schematically in figure 4.

The P-wave is associated with the depolarization of the atria and therefore the width of this wave is related to the size of the atria and the conduction speed of the action potential through the atrial tissue. This conduction speed and size are assumed to be proportional to the conduction speed and size of the ventricles. Consequently, the width of the P-wave window is set proportional to the width of the QRS complex, which is associated with the conduction of the depolarization front through the ventricles. The onset of the P-wave window is determined by the length of the PR interval (figure 3), which depends on the conduction speed through the AV node. As this conduction speed is regulated by the autonomous nervous system (Guyton and Hall 2000) and this system is also responsible for heart rate variability, the onset of the P-wave window is set dependent on the instantaneous maternal heart rate.

Definition of the window for detecting the T-wave is analogous to the definition of the P-wave window. The main difference is that the length of the RT interval, and thus the onset

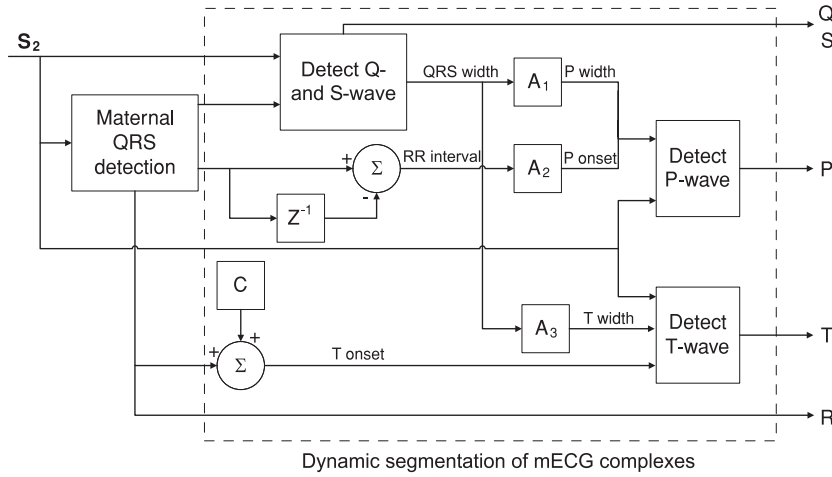


Figure 4. Block scheme of the mECG segmentation. The constants A_1 , A_2 , and A_3 are proportionality constants while the constant C represents a fixed delay between the QRS complex and the start of the T-wave.

of the T-wave window, is set at a fixed value C as the length of this interval is not regulated by neural stimulation. The width of the T-wave window is related to the repolarization of the ventricular tissues and is set proportional to the width of the QRS complex.

The windows for detecting the Q-, R- and S-wave are set at fixed values assuming no cardiac pathology like bundle branch blocks. These fixed values are chosen small enough to enable WAMES to deal with high maternal heart rates adequately.

Ideally, the start and end of each wave are detected in the windows as the first local extrema on either side of the peak. However, generally the P-wave and T-wave have a low SNR and, consequently, the detection of the start and end of the wave is less accurate. By defining an adaptive threshold that depends on the SNR within the window and performing the detection of the local extrema for the samples that do not exceed this threshold, the accuracy of this detection can be improved. The SNR within the window is approximated as the mean modulus of samples with moduli smaller than the mean modulus of all samples within the window.

Samples that are not detected in the individual ECG waves are included in the isoelectrical periods. These periods are associated with zero amplitude of the dipole or perpendicular orientation of the measurement vector with respect to the electrical field.

2.2. Linear prediction of maternal ECG segments

2.2.1. Alignment and scaling. Each wave in the mECG is estimated by the weighted averaging of N corresponding waves in preceding mECG complexes. Prior to averaging, the waves are aligned by synchronization on the start of the wave. As a result of the robustness in the mECG segmentation, however, the accuracy of the segmentation is not optimal and hence this alignment can be inaccurate up to a few sampling period. To improve the alignment the waves are synchronized by minimizing the mean squared error (MSE)

$$\theta_{\min} = \arg \min_{\theta_{i-k}} \frac{1}{M} \sum_{j=1}^M (Z_{i,j} - Z_{i-k,j+\theta_{i-k}})^2, \quad \theta_{i-k} \in \mathbb{Z}, \quad (5)$$

with M the length of the wave, θ_{i-k} the integer shift, $Z_{i,j}$ the wave that is estimated and $Z_{i-k,j}$ the corresponding wave of the k th preceding mECG complex ($Z = \{P, Q, R, S, T, iso\}$, $iso =$ isoelectrical period). Hereby, for each i and k the value of M is set equal to the shortest length of the waves $Z_{i,j}$ and $Z_{i-k,j}$. Hence, for longer waves only part of the wave is estimated. However, as in practice the lengths of the waves vary only gradually, this omission has a negligible effect. Each of the preceding waves $Z_{i-k,j}$ is thus shifted over a length θ_{\min} corresponding to the minimum MSE for that particular wave.

Due to respiration the dc component and amplitude of $Z_{i-k,j}$ differ from the dc component and amplitude of $Z_{i,j}$. Moreover, because of the finite sampling frequency (1 kHz, see section 4.1), misalignments smaller than one sampling period are expected, further decreasing the accuracy of the estimation. To improve accuracy, the dc component and amplitude of $Z_{i-k,j}$ have to be scaled properly and the time-shift (5) has to be extended with shifts smaller than one sampling period. To calculate the optimal parameters, in a least mean squared error sense, $Z_{i-k,j}$ require interpolation to obtain quasi-continuous signals. In this paper a parabolic interpolation scheme is used, i.e., for each sample a parabola is fitted through that particular sample and the adjacent samples on either side

$$\tilde{Z}_{i-k,j} = \alpha_j j^2 + \beta_j j + \gamma_j. \quad (6)$$

Here $\tilde{Z}_{i-k,j}$ is the interpolated wave and α_j , β_j and γ_j are the parabolic coefficients. The reason for using parabolic interpolation is that it is the lowest order polynomial interpolation that can account for local extrema and has a continuous first derivative. Moreover, its computational simplicity is favored over more complex interpolation schemes. The time-shifted, dc offset compensated, and scaled wave $Z'_{i-k,j}$ can be calculated by

$$Z'_{i-k,j} = a\tilde{Z}_{i-k,j+b} + c, \quad (7)$$

$$a \in \mathbb{R}, \quad b \in \{\mathbb{R} \cap (-\Delta t_s, \Delta t_s)\}, \quad c \in \mathbb{R}, \quad (8)$$

with a the scaling parameter, b the required time-shift, c the dc component and Δt_s the length of one sampling period. It has to be noted here that, as $\tilde{Z}_{i-k,j}$ is an interpolated wave, $Z'_{i-k,j}$ is an interpolated wave as well. The optimal parameters \hat{a} , \hat{b} and \hat{c} are calculated by minimizing the MSE between the estimated wave $Z_{i,j}$ and the time-shifted, offset compensated, scaled and interpolated wave $Z'_{i-k,j}$

$$\vec{\nabla} \left(\frac{1}{M'} \sum_{j \in F_{i-k}} (Z_{i,j} - Z'_{i-k,j})^2 \right) = \vec{0}, \quad (9)$$

where $\vec{\nabla}$ stands for the gradient $(\frac{\partial}{\partial a}, \frac{\partial}{\partial b}, \frac{\partial}{\partial c})$. Here F_{i-k} is the set of samples that do not contain artifacts of fECG complexes and M' is the number of samples included in F_{i-k} .

Artifacts and fECG complexes affect the calculation of the parameters \hat{a} , \hat{b} and \hat{c} and therefore reduce the accuracy of the mECG estimation. By excluding samples that possibly contain artifacts and fECG complexes from the calculation of these parameters, the accuracy can be improved (Vullings *et al* 2007). Artifacts and fECG complexes generally distort the mECG wave. Comparison of waves with normalized amplitudes provides information about the rate of distortion and consequently enables detection of samples containing artifacts or fECG complexes (Vullings *et al* 2007).

2.2.2. Prediction. The waves $Z_{i,j}$ in the mECG are estimated by the weighted averaging of the aligned and scaled waves of preceding mECG complexes $Z'_{i-k,j}$ (8). The weights used in

this averaging are determined as the reciprocals of the MSE

$$w_{i-k} = \left(\frac{1}{M'} \sum_{j \in F_{i-k}} (Z_{i,j} - Z'_{i-k,j})^2 \right)^{-1}. \quad (10)$$

Since several preceding waves are included in the averaging, it can occur that both $Z_{i,j}$ and $Z_{i-k,j}$ for a particular k are similarly distorted by a fECG complex. Consequently, exclusion of samples from F_{i-k} can be erroneous and as a result the weight w_{i-k} can be too large, i.e., a similar distortion of $Z_{i,j}$ and $Z_{i-k,j}$ causes the MSE to be relatively small and hence the weight to be relatively large. Furthermore, it can occur that preceding waves suffer from large distortions, resulting in relatively small weights w_{i-k} . These waves, however, still affect the averaged estimate of $Z_{i,j}$. To overcome these effects, only preceding waves are included in the weighted averaging for which the weights w_{i-k} are in the interval

$$\bar{w} - \sigma_w \leq w_{i-k} \leq \bar{w} + \sigma_w, \quad (11)$$

with \bar{w} the mean weight and σ_w the square root of the weight variance.

The average mECG wave $\hat{Z}_{i,j}$ can subsequently be calculated by

$$\hat{Z}_{i,j} = \frac{\sum_{k \in G} w_{i-k} Z'_{i-k,j}}{\sum_{k \in G} w_{i-k}}. \quad (12)$$

Here, G is the set of preceding waves with weights satisfying (11). The maximum number of waves in G is restricted to the number of preceding waves N included in the estimation of the mECG. Assuming that the fECG and mECG are not synchronized and disregarding the scaling of the waves, the amplitude of the fECG in the average mECG wave $\hat{Z}_{i,j}$ is reduced by a factor equal to the number of waves included in G . The desired reduction of the fECG amplitude in the averaging is empirically set at 10. Since only preceding waves with weights satisfying (11) are included in the averaging, the number of preceding waves N included in the estimation has to exceed 10. Assuming a normal distribution of the weights, applying (11) results in $N = 15$.

2.3. Maternal ECG segment combination

As the waves Z_{ij} are estimated independently from each other, combination of the individual estimates $\hat{Z}_{i,j}$ into an estimate of the mECG signal \hat{S}_2 (figure 2) can result in discontinuities at the segment transitions due to different dc offsets. To avoid this, linear interpolation is applied on the segment transitions. This interpolation is performed in an interval of 10 ms centered around the actual segment transition.

3. Other methods for maternal ECG removal

Several other techniques are implemented in the mECG cancellation block of figure 1 for comparison to WAMES. These techniques are discussed briefly in this section. In addition, the performance of WAMES in fHR detection is compared to the performance of ICA and hence ICA is discussed in this section as well.

3.1. Spatial filtering

By regarding the abdominal mECG as a superposition of three independent and orthogonal sources, three independent signals V_1 , V_2 and V_3 are sufficient to construct a fourth mECG signal V_4 (Bergveld and Meijer 1981)

$$V_4 = \lambda_1 V_1 + \lambda_2 V_2 + \lambda_3 V_3. \quad (13)$$

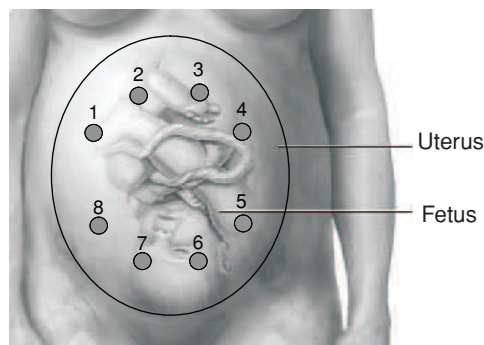


Figure 5. Electrode configuration on the maternal abdomen.

The coefficients λ_1 , λ_2 and λ_3 can be estimated by $\hat{\lambda}_1$, $\hat{\lambda}_2$ and $\hat{\lambda}_3$ by using the optimization procedure of Hildreth and d'Esopo (Künzi and Krelle 1962).

According to Bergveld and Meijer (1981) the estimated coefficients are stable for 4 s. Consequently, the optimization procedure is repeatedly applied on signal windows of 4 s. Moreover, the information contained in three signals appeared to be insufficient for all recordings (Bergveld and Meijer 1981), resulting in a suboptimal estimation of V_4 . For this reason, in this paper (13) is extended to eight signals V_i with $i = \{1, \dots, 8\}$; each of the eight recorded signals (figure 5) is estimated using the other seven signals. The reason for extending (13) to eight signals is the employed electrode configuration consisting of eight abdominal electrodes; this configuration is discussed in section 4.

3.2. Adaptive filtering

Noise canceling is a variation of adaptive filtering that can be highly advantageous for mECG removal in antenatal abdominal recordings (Widrow *et al* 1975). Adaptive noise cancellers (ANC) build a reference mECG and subtract this from the abdominal recordings that contain both mECG and fECG. As a result, the mECG is attenuated whereas the fECG remains unaffected. By using an artificial reference, generated by the event-triggered averaging of mECG complexes, problems arising by the nonlinear propagation of the mECG can be overcome (Strobach *et al* 1994). In the case of antenatal abdominal recordings this means that a mECG template is generated by averaging several consecutive mECG complexes, synchronized on the QRS complex. This mECG template is subsequently used as a reference signal in the ANC; this technique is referred to as event synchronous adaptive interference canceling (ESAIC) and implemented as described in Strobach *et al* (1994).

3.3. Template subtraction

Standard template subtraction techniques generate a mECG template for the complete mECG complex by event synchronous averaging, i.e. before averaging the mECG complexes are synchronized on the QRS complexes. This template is subsequently linearly scaled to minimize the MSE with respect to the mECG complex that is estimated and subtracted (Cerutti *et al* 1986).

Two different techniques to further improve this template and to generate this template are mentioned in the literature: the event synchronous interference canceller (ESC) (Ungureanu

and Wolf 2006, Martens *et al* 2007) and linear prediction (LP) (Ungureanu *et al* 2007, Comani *et al* 2004), respectively.

3.3.1. Event synchronous interference canceling. As respiration can cause variation in the amplitude of the mECG complex, gain adaption is preferred within each mECG complex (Martens *et al* 2007, Ungureanu and Wolf 2006), i.e., the template is segmented and the required linear scaling is calculated for each segment separately. Implementation of ESC is performed according to Ungureanu and Wolf (2006); segmentation of the template is performed similar to WAMES, as detailed in section 2.1.

3.3.2. Linear prediction. After synchronization on the QRS complexes, for LP, the mECG complexes are not averaged like for the ESC (with equal weights), but rather are the weights for the averaging calculated to minimize the MSE. Hence, the mECG complex \hat{V}_i can be estimated by the linear combination of preceding mECG complexes \vec{V}_{i-k} with weights λ_{i-k}

$$\hat{V}_i = \sum_{k=1}^K \lambda_{i-k} \vec{V}_{i-k}, \quad (14)$$

with K the order of the prediction model. By minimizing the MSE between the estimate \hat{V}_i and the actual mECG complex \vec{V}_i the weights $\vec{\lambda}_i = [\lambda_{i-1}, \dots, \lambda_{i-K}]^T$ can be calculated

$$\vec{\lambda}_i = (\mathbf{V}_i^T \mathbf{V}_i)^{-1} \mathbf{V}_i^T \vec{V}_i \quad (15)$$

with $\mathbf{V}_i = [\vec{V}_{i-1}, \dots, \vec{V}_{i-K}]^T$. Implementation of LP is performed according to Ungureanu *et al* (2007) and hence K is set at 7.

3.3.3. Main differences with WAMES. As WAMES is based on template subtraction as well, both ESC and LP resemble WAMES to some extent. However, the main differences with ESC are that with WAMES the scaling of interpolated segments is performed before averaging, while ESC does not use interpolation and generates an average template before scaling its segments. Moreover, synchronizing of the segments in WAMES is not based on synchronization of the QRS complexes, but rather on minimizing the MSE between the separate segments. Finally, in WAMES samples containing possible fECG complexes or artifacts are excluded from scaling parameter calculations and not all preceding segments are included in the averaging (11). All these differences serve to increase the accuracy of mECG estimation.

With respect to ESC, WAMES and LP are more different. LP does not use segmentation and artifact exclusion. Moreover, the weights for averaging in LP are determined on a minimum MSE basis while this approach is not beneficial for WAMES; due to segmentation, the contribution of noise in the weight calculation for the separate segments is too large, resulting in a reduced performance in the mECG estimation.

3.4. Independent component analysis

ICA is a statistical signal processing technique for separating observed signal mixtures into latent source signals. Given a set of observed signals \mathbf{X} and assuming that this set is generated by the statistically independent source signals \mathbf{Y} , it can be stated that (Comon 1994)

$$\mathbf{X} = \mathbf{A}\mathbf{Y} + \mathbf{N}. \quad (16)$$

Here \mathbf{A} is a constant full-rank matrix, referred to as the mixing matrix and \mathbf{N} is additive noise.

The goal of ICA is to estimate the independent source signals matrix \mathbf{Y} , or equivalently, to estimate the mixing matrix \mathbf{A} . When ICA is applied to antenatal abdominal recordings, the observed signals \mathbf{X} are represented by the preprocessed signals \mathbf{S}_2 (figure 1) and the independent source signals \mathbf{Y} are represented by, among others, the fECG and mECG.

To account for non-stationarities in the mixing matrix \mathbf{A} due to, e.g. fetal movement, ICA is repeatedly applied on temporal windows of \mathbf{S}_2 with length of 4 s (section 3.1), i.e. for each 4 s of data ICA is applied on the observed signals, resulting in a mixing matrix \mathbf{A} that is updated every 4 s.

Restriction of ICA is that the order of the independent signals cannot be controlled and as a result, in consecutive calculations the source signals can be swapped. To overcome this signal swapping problem, half-overlapping windows are used in combination with a correlation scheme to re-order the independent signals (Taylor *et al* 2003).

The independent source signal representing the fECG is selected automatically based on a physiological model of the fHR (Abboud and Sadeh 1990). Independent source signals representing the mECG but satisfying this model are excluded based on maternal heart rate information obtained through detection of the maternal QRS complexes in the recorded signals. When none of the independent signals satisfies the physiological fHR model, the window length used for the input signals of ICA is adapted; large non-stationarities can require shorter windows whereas estimation of a stationary mixing matrix is improved when the window length is enlarged.

For implementation of ICA the Joint Approximate Diagonalization of Eigenmatrices (JADE) algorithm (Cardoso and Souloumiac 1993) is employed; a non-Gaussianity based solution to the ICA problem.

4. Data and methodology for comparison

The performance of WAMES in estimating the mECG is assessed by comparison with the performance of other techniques on modeled antenatal abdominal recordings. Reason for using modeled recordings is that in real abdominal recordings, the mECG is affected by noise and fECG and hence the absolute performance cannot be assessed quantitatively.

In addition, the performance of WAMES in fHR detection is assessed by comparing the performance to the performance of other techniques on real antenatal abdominal recordings. The detected fHR values are validated by comparison to the fHR detected from a simultaneously performed invasive fECG recording from the fetal scalp.

4.1. Data acquisition and modeling

The abdominal recordings are conducted with a M-PAQ amplifier (Maastricht Instruments B.V., the Netherlands), a 16 channel system for physiological measurements with programmable gain and sampling frequency and high input impedance ($10^8 \Omega$). For the abdominal recordings the gain is set at 500 and the sampling frequency at 1 kHz.

The adopted electrode configuration consists of eight unipolar contact electrodes on the maternal abdomen with a common reference as shown in figure 5. This configuration has been chosen since it covers most of the uterine surface, while patient discomfort, resulting from too many electrodes, is minimized.

4.1.1. Modeling antenatal abdominal recordings. Ten eight-channel abdominal recordings of 60 s each are performed on a non-pregnant subject with the electrode configuration of figure 5. To model antenatal abdominal recordings, a fECG signal recorded directly from

the fetal scalp during parturition and a Gaussian white noise source are superimposed on the mECG recordings. Note that this model is not an accurate representation of actual antenatal abdominal recordings. However, it is suitable for the assessment of the mECG removal performance.

For each eight-channel recording, 49 modeled antenatal abdominal recordings are generated having different amplitude ratios between the mECG, fECG and Gaussian noise. Moreover, the fact that the models are generated using ten different abdominal recordings ensures that the models comprise different degrees of variability in the mECG morphology.

The amplitude ratios between mECG, fECG and noise are defined as the ratio between the root mean squared (RMS) amplitudes. The employed mECG to noise amplitude ratios range from 7 dB to 17 dB and the employed mECG to fECG amplitude ratios range from 3 dB to 13 dB. Finally, the morphological variability of the different abdominal recordings ranges from 0.15 to 0.32. This variability is defined as the RMS error between the normalized mECG complexes and an mECG template, generated by averaging the normalized mECG complexes.

4.1.2. Real antenatal abdominal recordings. Seven eight-channel antenatal abdominal recordings of 10 min each are performed on pregnant subjects during parturition with the electrode configuration of figure 5. In addition, the direct fECG is recorded simultaneously by an electrode positioned on the fetal scalp and passed on to the M-PAQ through the analog output of an HP8040 fetal monitor (Hewlett-Packard).

The patients have gestational ages ranging from 37 to 41 weeks and the medical indication for the group varies from healthy to preexistent hypertension and preeclampsia.

4.2. Preprocessing

As stated previously, antenatal abdominal recordings generally constitute a mixture of fECG, mECG and interferences such as motion artifacts, muscular activity and powerline interference. In preprocessing the abdominal recordings of each of these interferences is suppressed by means of applying a linear-phase filter.

Motion artifacts are suppressed by a 1000 tap FIR high-pass filter with fixed cutoff frequency of 1.5 Hz. This cutoff frequency maximizes the suppression of the artifacts while minimizing distortion of the fECG signals. The powerline interference is centered around 50 Hz and suppressed by a 1000 tap FIR notch filter with stop-band between 49 and 51 Hz. Harmonics of the powerline interference and part of the noise originating from muscular activity (electromyogram, EMG) are suppressed by a 1000 tap FIR low-pass filter with fixed cutoff at 70 Hz. As the EMG exhibits spectral properties ranging from 0 to 200 Hz this filter only suppresses part of the EMG. However, as the frequency range of the fECG is limited by a upper bound of 70 Hz (Abboud and Sadeh 1989), a lower cutoff frequency would result in distortion of the fECG.

4.3. Methodology of comparison

The performance of WAMES in estimating the mECG in the modeled antenatal abdominal recordings is compared to the performance of spatial filtering, ESAIC, ESC and LP by assessing the normalized MSE ϵ between \mathbf{S}_2 and $\hat{\mathbf{S}}_2$ (figure 2)

$$\epsilon = \frac{\sum_n [\mathbf{S}_2(n) - \hat{\mathbf{S}}_2(n)]^2}{\sum_n [\mathbf{S}_2(n)]^2}. \quad (17)$$

In addition, the performance of WAMES is compared to ICA by assessing the fHR detection in real antenatal abdominal recordings. The detection of the fHR is performed by

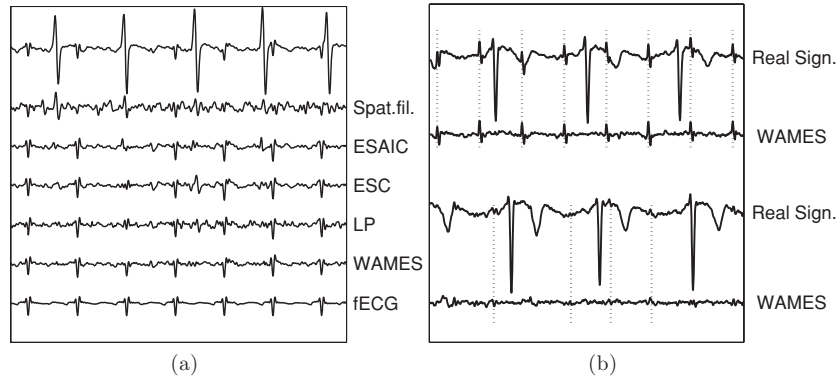


Figure 6. Results of mECG subtraction on (a) modeled antenatal abdominal recordings and (b) preprocessed real antenatal abdominal recordings. The mECG subtraction in (a) is performed by spatial filtering, ESAIC, ESC, LP and WAMES. The upper graph shows the modeled antenatal abdominal recording with mECG to noise ratio 17 dB and mECG to fECG ratio 6 dB. The five centered graphs show the resulting signals after subtraction of the mECG estimates. The bottom graph shows the fECG signal used in the modeled abdominal recording. The mECG subtraction in (b) is performed by WAMES alone and comprises a best-case scenario in the upper two graphs and a worst-case scenario in the bottom two graphs. The dotted lines indicate the positions of detected fetal QRS complexes. Note that for the worst-case scenario the peaks are detected in the principal component which, in contrast to the real signal shown, does exhibit some fECG signal.

calculating the interval lengths between consecutive fetal QRS complexes. In the independent source signal representing the fECG the QRS complexes are detected as described in section 2.1.1, i.e. as local extrema exceeding a variable threshold.

Detection of the fHR in the signals obtained by mECG removal through WAMES is not as straightforward as detection of the fHR in the independent source signals; in contrast to ICA, WAMES provides an fECG signal for each recorded signal. Through PCA the inter-channel correlation of these fECG signals can be exploited, performing the previously described fHR detection method on the principal component and hence solving this problem.

Performance of the fHR detection by both WAMES and ICA is assessed by the sensitivity Se and the positive predictive value PPV

$$Se\% = \frac{TP}{TP + FN} \cdot 100, \quad (18)$$

$$PPV\% = \frac{TP}{TP + FP} \cdot 100. \quad (19)$$

Here TP is the number of correctly detected fetal QRS complexes, FN the number of undetected QRS complexes and FP the number of falsely detected QRS complexes. The golden standard to establish whether fetal QRS complexes are correctly detected or missed are the QRS complexes detected from the simultaneously recorded fECG signal from the fetal scalp.

5. Results and discussion

5.1. Comparison on mECG estimation

Figure 6(a) shows a modeled antenatal abdominal recording and the signals resulting after subtraction of the mECG estimates by the different techniques. The depicted signals comprise

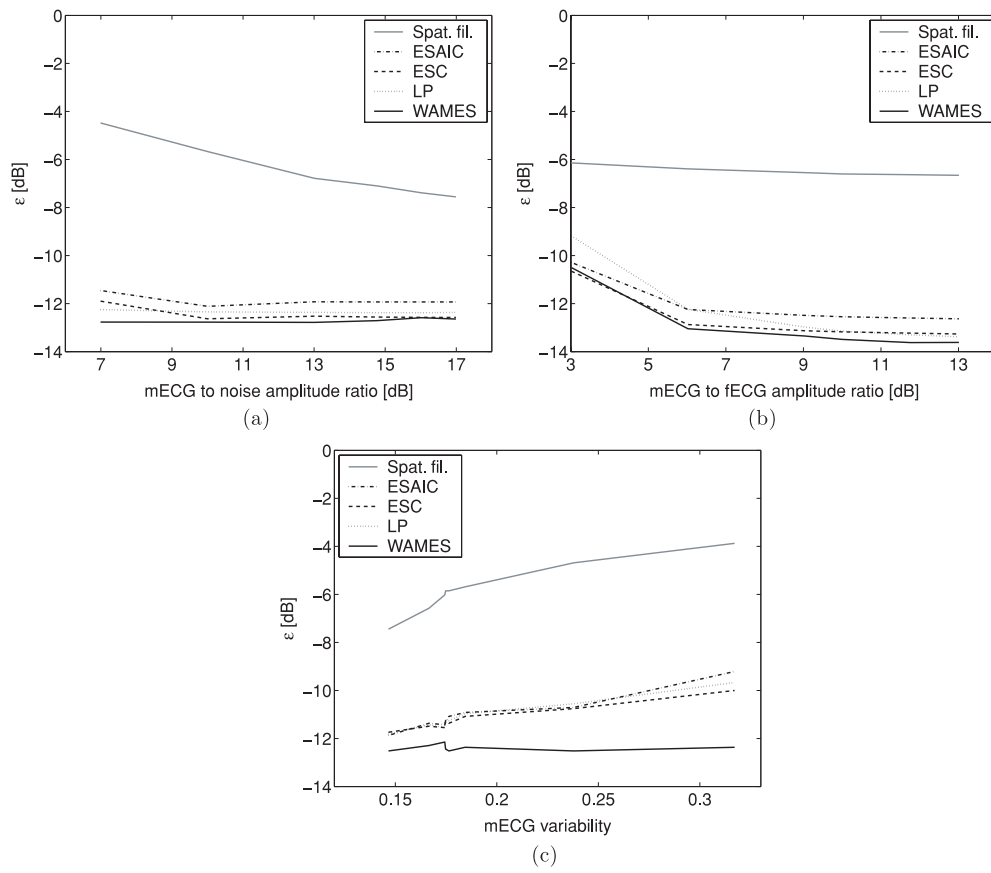


Figure 7. Normalized mean squared error ϵ between the mECG used in the modeled antenatal abdominal recordings and the estimate of this mECG for (a) different mECG to noise amplitude ratios, (b) different mECG to fECG amplitude ratios and (c) different degrees of mECG morphological variability. For each plot the values of ϵ are obtained by averaging over the other dimensions, e.g. for (a) the values of ϵ are obtained by averaging over all mECG to fECG amplitude ratios and mECG variability values.

3 s of a 60 s recording. To evaluate the modeled antenatal abdominal recordings with respect to real recordings, in figure 6(b) the subtraction of mECG estimates by WAMES on real antenatal abdominal recordings is depicted. Figure 7 shows ϵ for different amplitude ratios between the mECG, the fECG and the noise and for different degrees of variability in the mECG morphology.

The results depicted in figure 7 show that WAMES performs better in subtracting the mECG than spatial filtering, ESAIC, ESC and LP for almost all modeled antenatal abdominal recordings. Moreover, although the differences in performance by WAMES on the one hand and ESAIC, ESC and LP on the other hand appear to be small, in particular for figures 7(a) and (b), even these small differences in performance can be of major significance. The error in the mECG subtraction is generally of the same order of magnitude as the fECG, especially in early stages of pregnancy, and hence it can significantly corrupt the remaining fECG signal.

For recordings with a small mECG to fECG amplitude ratio, i.e. a large fECG signal, WAMES underperforms ESC. The large amplitude of the fECG complexes causes

Table 1. Performance assessment of the detection of fetal QRS complexes. The values in this table represent percentages (%).

	Se	σ_{Se}	Range	PPV	σ_{PPV}	Range
Spat. fil.	82.7	3.4	80.0–90.4	91.6	2.8	85.7–94.1
ESAIC	89.8	3.6	87.2–97.2	94.2	2.8	88.4–96.7
ESC	90.1	3.5	87.6–97.5	94.4	2.7	88.9–96.8
LP	90.1	4.0	86.3–97.6	94.2	2.8	88.7–98.9
ICA	91.8	4.0	88.2–99.4	94.8	2.6	89.6–97.3
WAMES	94.8	3.7	89.6–99.3	95.1	1.8	92.5–97.7

significant inaccuracies in the mECG segmentation, resulting in a decreased accuracy of mECG estimation. Since ESC performs segmentation after averaging of consecutive mECG complexes, the fECG amplitude is reduced in this average mECG complex and hence the segmentation is affected to a smaller extent. It has to be remarked, though, that this mECG to fECG amplitude ratio is not commonly encountered in medical practice.

Increased variability in the mECG morphology causes no significant difference in estimation error ϵ for WAMES. In contrast, the other techniques suffer from an increased ϵ with increasing variability.

5.2. Comparison on fetal heart rate detection

In total 70 min of data is analyzed, containing 10^4 fetal QRS complexes. The performance of the detection of these complexes by the aforementioned techniques including ICA is presented in table 1, in which Se and PPV are the values averaged over the seven recordings, σ_{Se} and σ_{PPV} are the standard deviations, and range indicates the minimum and maximum values.

The results presented in table 1 show that the performance of WAMES in detecting the fHR is slightly better than the performance of the other techniques; the Se of WAMES is 3% larger than the Se of the second best technique (ICA). The PPV of WAMES is nearly equal to the PPV of the other techniques.

5.3. Discussion

In general, WAMES performs better in mECG subtraction and fHR detection than the other techniques. At first, the 3% difference with ICA might seem rather small. However, since WAMES provides spatial information on the fECG, whereas ICA cannot provide this information unless three independent fECG sources are determined, this 3% difference should be considered as an additional advantage.

Notwithstanding this advantage of WAMES, in cases of maternal ectopic beats, WAMES is expected to underperform in removing the mECG and detecting the fHR with respect to ICA. WAMES is incapable of handling the additional mECG complexes sufficiently accurately as WAMES assumes only small variations in the mECG morphology.

Moreover, subtraction of the estimated mECG signal by WAMES is analogous to the superposition of an error signal to the fECG signal. This error signal constitutes the difference between the mECG and the mECG estimate, and generally has a peaky nature. For recordings with a smaller fECG amplitude, i.e., recordings in stages of pregnancy much earlier than labor, these peaks can be expected to have the same order of magnitude as the fECG and hence might affect the performance of WAMES. For these recordings the fHR detection by ICA is

therefore expected to outperform the fHR detection by WAMES. In future implementations of fHR detection methods it can, however, be advantageous to use WAMES as preprocessing step for ICA, exploiting the strong features of both techniques.

A final remark about the presented fHR detection performances can be made by stating that these results can be improved by applying a dedicated fetal QRS detection method instead of the method discussed in section 2.1.1.

6. Conclusions

In this paper, a new technique (WAMES) is presented to remove the mECG from antenatal abdominal recordings in order to extract the fECG and fHR. WAMES is compared to several other mECG removal techniques, namely, spatial filtering, ESAIC, ESC and LP. Moreover, the suitability of WAMES for fHR monitoring is assessed by comparing the performance in detecting the fetal QRS complexes to the performance of the aforementioned techniques plus ICA. WAMES proves to be more accurate in mECG removal than the other techniques and performs also better in fHR detection. In addition, implementations of WAMES in Matlab[®] (The Mathworks, Inc.) on a laptop computer with a 1.7 GHz Pentium[®] processor show that the mECG can be removed in real time. This implementation is executed on a clinical prototype, NEMO, that is currently evaluated in the Máxima Medical Center, the Netherlands. Provisional experience of clinicians is very positive; the added value of the fECG and spectral analysis of the fHR, however, still needs to be further investigated.

Although WAMES outperforms the other techniques in mECG subtraction, the differences in performance by WAMES and the other techniques appear to be rather small. However, in clinical practice the variability in the mECG morphology is significantly larger than the variability in the recordings used in this study. The reason for this is that the subjects participating in this study were, due to ethical considerations, in general healthy women lying in a comfortable position during the recordings. However, in practice, the most relevant cases are those pregnancies where either mother or fetus is suffering from illness or distress and consequently the mother is not lying comfortable and still anymore. In these situations the mECG morphological variability is expected to be 0.25 or larger (figure 7(c)) and, as a result, the performance of WAMES is expected to improve with respect to the other techniques.

In conclusion, it can be stated that WAMES provides a tool for mECG removal in antenatal abdominal recordings for which the performance is relatively insensitive to noise and variability in the mECG morphology. When the main interest for mECG removal is monitoring of the fHR, no conclusive statement can be made whether WAMES should be preferred over the other techniques as the available amount of abdominal recordings is not sufficient to render statistical significance. However, for the recordings that are available, WAMES slightly outperforms the other techniques. When the aim is to monitor and analyze the fECG, WAMES is preferred over the other techniques as it provides relatively accurate spatial information on the fECG, possibly enabling future implementations of fetal vectorcardiography.

Future research, besides the combined employment of WAMES and ICA, fetal vectorcardiography and development of a dedicated fetal QRS detection method, includes extraction and enhancement of fECG complexes and assessment of the performance of WAMES in cases of maternal or fetal pathology.

Acknowledgment

This work was supported by the Dutch Technology Foundation STW.

References

- Abbound S and Sadeh D 1989 Spectral analysis of the fetal electrocardiogram *Comput. Biol. Med.* **19** 409–15
- Abbound S and Sadeh D 1990 Power spectrum analysis of fetal heart rate variability using the abdominal maternal electrocardiogram *J. Biomed. Eng.* **12** 161–4
- Amer-Wahlin I *et al* 2001 Cardiotocography only versus cardiotocography plus ST analysis of fetal electrocardiogram for intrapartum fetal monitoring: a Swedish randomised controlled trial *Lancet* **18** 534–8
- Bemmel J H V and van der Weide H 1966 Detection procedure to represent the foetal heart rate and electrocardiogram *IEEE Trans. Biomed. Eng.* **13** 175–82
- Bergveld P and Meijer W J H 1981 New technique for the suppression of the MECG *IEEE Trans. Biomed. Eng.* **28** 248–353
- Cardoso J F and Souloumiac A 1993 Blind beamforming for nonGaussian signals *IEE Proc.-F* **140** 362–70
- Cerutti S, Baselli G, Civardi S, Ferrazzi E, Marconi A M, Pagani M and Pardi G 1986 Variability analysis of fetal heart rate signals as obtained from abdominal electrocardiographic recordings *J. Perinat. Med.* **14** 445–52
- Comani S, Mantini D, Lagatta A, Esposito F, Luzio S D and Romani G L 2004 Time course reconstruction of fetal cardiac signals from fmcg: independent component analysis versus adaptive maternal beat subtraction *Physiol. Meas.* **25** 1305–21
- Comon P 1994 Independent component analysis, a new concept? *Signal Process.* **36** 287–314
- Dawes G, Visser G, Goodman J and Redman C 1981 Numerical analysis of the human fetal heart rate: the quality of ultrasound records *Am. J. Obstet. Gynecol.* **141** 43–52
- De Lathauwer L, Moor B D and Vanderwalle J 2000 Fetal electrocardiogram extraction by blind source subspace separation *IEEE Trans. Biomed. Eng.* **47** 567–72
- Greene K, Dawes G, Lilja H and Rosén K 1982 Changes in the ST waveform of the fetal lamb electrocardiogram with hypoxemia *Am. J. Obstet. Gynecol.* **144** 950–8
- Gritzali F, Frangakis G and Papakonstantinou G 1989 Detection of the P and T waves in an ECG *Comput. Biomed. Res.* **22** 83–91
- Guyton A and Hall J 2000 *Textbook of Medical Physiology* 10th edn (Philadelphia, PA: WB Saunders)
- Künzi H and Krelle W 1962 *Nichtlineare Programmierung* (Berlin: Springer)
- Lawson G, Belcher R, Dawes G and Redman C 1983 A comparison of ultrasound (with autocorrelation) and direct electrocardiogram fetal heart rate detector systems *Am. J. Obstet. Gynecol.* **147** 721–2
- Martens S, Rabotti C, Mischi M and Sluijter R 2007 A robust fetal ECG detection method for abdominal recordings *Physiol. Meas.* **28** 373–88
- Martens S, Sluijter R, Oei S and Bergmans J 2005 Improving QRS detection in multi-channel electrocardiography by principal component analysis *IFMBE Proc. (Prague, Czech Republic)*
- Plonsey R 1969 *Bioelectric Phenomena* (New York: McGraw-Hill)
- Siira S, Ojala T, Vahlberg T, Jalonen J, Välimäki I, Rosén K and Ekholm E 2005 Marked fetal acidosis and specific changes in power spectrum analysis of fetal heart rate variability recorded during the last hour of labour *BJOG* **112** 418–23
- Stinstra J *et al* 2002 Multicentre study of fetal cardiac time intervals using magnetocardiography *BJOG* **109** 1235–43
- Strobach P, Abraham-Fuchs K and Härer W 1994 Event-synchronous cancellation of the heart interference in biomedical signals *IEEE Trans. Biomed. Eng.* **41** 343–50
- Taylor M, Smith M, Thomas M, Green A R, Cheng F, Oseku-Afful S, Wee L Y, Fisk N M and Gardiner H M 2003 Non-invasive fetal electrocardiography in singleton and multiple pregnancies *BJOG* **110** 668–78
- Thacker S, Stroup D and Chang M 2001 Continuous electronic heart rate monitoring for fetal assessment during labor *Cochrane Database Syst. Rev.* **3** CD000063
- Ungureanu M, Bergmans J, Oei S and Strungaru R 2007 Fetal ECG extraction using an adaptive maternal beat subtraction technique *Biomed. Tech.* **52** 56–60
- Ungureanu M and Wolf W 2006 Basic aspects concerning the event-synchronous interference canceller *IEEE Trans. Biomed. Eng.* **53** 2240–7
- Van Laar J, Porath M, Peters C and Oei S 2008 Spectral analysis of fetal heart rate variability for fetal surveillance: a review of the literature *Acta Obstet. Gynecol. Scand.* **87** 300–6
- Vullings R, Peters C, Mischi M, Sluijter R, Oei G and Bergmans J 2007 Artifact reduction in maternal abdominal ECG recordings for fetal ECG estimation *Proc. of IEEE EMBC (Lyon, France)* pp 43–6
- Widrow B, Glover J R, McCool J, Kaunitz J, Williams C S, Hearn R H, Zeidler J R, Dong E and Goodlin R 1975 Adaptive noise cancelling: principles and applications *Proc. IEEE* **62** 1692–716
- Zarzoso V and Nandi A 2001 Noninvasive fetal electrocardiogram extraction: blind separation versus adaptive noise cancellation *IEEE Trans. Biomed. Eng.* **48** 12–8